THE INTERNATIONAL JOURNAL OF SCIENCE & TECHNOLEDGE

Automobile Battery Monitoring System using Arduino Uno R3 Microcontroller Board

Ignatius Nakhoywa Barasa
Graduate Researcher, Department of Physics, University of Nairobi, Nairobi, Kenya
Justus Simiyu
Senior Lecturer, Department of Physics, University of Nairobi, Nairobi, Kenya
Sebastian Waita
Senior Lecturer, Department of Physics, University of Nairobi, Nairobi, Kenya
Denis Wekesa
Final year Student, Department of Electrical and Electronics Engineering, University of Nairobi, Nairobi, Kenya
Bernard Aduda
Professor, Department of Physics, University of Nairobi, Nairobi, Kenya
Principal, College of Biological and Physical Science, University of Nairobi, Nairobi, Kenya

Abstract:
The car starter battery normally provides electrical power for engine cranking, lighting of accessories and feeding the engine ignition system. During any given car engine cranking event, a high current ranging from 100A to 1500A, depending on the engine capacity and starter motor type is usually drawn from the starter battery. With each engine cranking event, there is an associated voltage loss in the battery which consequently leads to battery degradation and ultimate failure. The failure may occur abruptly thereby inconveniencing and at times endangering the life of the motorist. The battery monitoring system in this research used the voltage loss associated with each engine cranking event to compute the state of health of the car starter battery. It has a voltage divider, current and temperature modules designed for measuring the battery's voltage, current and temperature respectively using a microcontroller on an Arduino Uno R3 computing board. Just before the engine cranking request is made, the battery temperature and open circuit voltage are recorded, followed by the set of current and voltage values drawn during engine cranking. After a successful engine cranking event, the acquired temperature compensated voltage value is subtracted from the open circuit voltage value to get the voltage loss for that particular cranking event. The voltage loss together with a voltage loss threshold value were then used in computing the cranking health status of battery and the result displayed in real time to the motorist over a screen on the car's dashboard. Of the 2 batteries used in the laboratory and in a car in this research, one of them needed to be replaced since its state of health fell below the state of health threshold while the other battery was in good cranking condition since it was brand new. The motorist in whose car this battery monitoring system is installed will be able to know beforehand about an impending battery failure and so take the necessary precaution in time.

Keywords: *State of health, State of charge, Arduino microcontroller, engine cranking event, lead acid battery*

1. Introduction

A battery is a device that converts the chemical energy stored in its active materials to electrical energy through an electrochemical reaction (Jung *et al.*, 2016).The active materials for the lead acid battery (LAB) are the lead oxide (PbO_2) and lead (Pb) terminal plates and a solution of sulfuric acid (H_2SO_4) (Rekioua and Matagne, 2012). The structure of a rechargeable lead acid is shown in Figure 1;

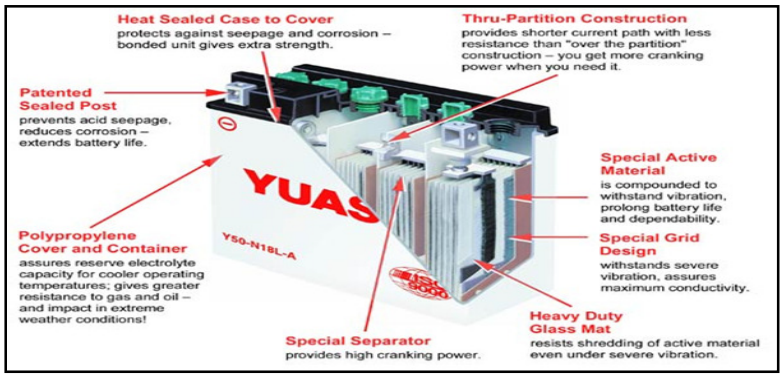

Figure 1: Structure of a typical rechargable lead acid battery (Yuasa, 2016)

The most prevalent battery technology, due to low internal resistance and low price is the LAB which is commonly used in cars for starting, lighting and ignition, functions that are otherwise known as (SLI). SLI batteries are designed with battery grids having minimum electrical resistance, thin plates and higher concentrations of electrolyte to maximize the cranking ability. Heavy-duty SLI batteries for trucks, buses and construction equipment use heavier and thicker plates which have high-density paste and premium separators that often have glass mat in them in order to enhance longer life.

2. Battery Monitoring

The battery's temperature, voltage, current and state of charge (SoC) are the most common parameters that are normally monitored. Currently, the number of electrical appliances in the modern car keep increasing and consequently the need for more power from the battery which can, if not monitored, easily and abruptly lead to battery failure thereby inconveniencing or endangering the motorist. There is need therefore, of a car battery monitoring system (BMS) for monitoring and relaying to the motorist, the real-time health status of the car's battery by providing reliable information and notification of its working condition and the appropriate action to be taken when need arises.

2.1. Background of a Battery Monitoring System

A BMS is an electronic device that measures specified battery parameters, analyzes them using pre-programmed instructions and relays the output to the end user most often over a screen. The monitoring of the state of health (SoH) of the car starter battery is still a big challenge due to the lack of sensors for the electrochemical phenomena inside the battery's cells (Dyer *et al.*, 2014). The accuracy of battery monitoring systems has always been a point of discussion as they generally give an error of about 10% when all the parameters and components of the BMS are put in consideration (Patil *et al*., 2011). Research is being undertaken by a group of researchers for embedding sensors inside the car starter battery to monitor individual cells as is shown in Figure 2 (Matthias *et al.,* 2015).

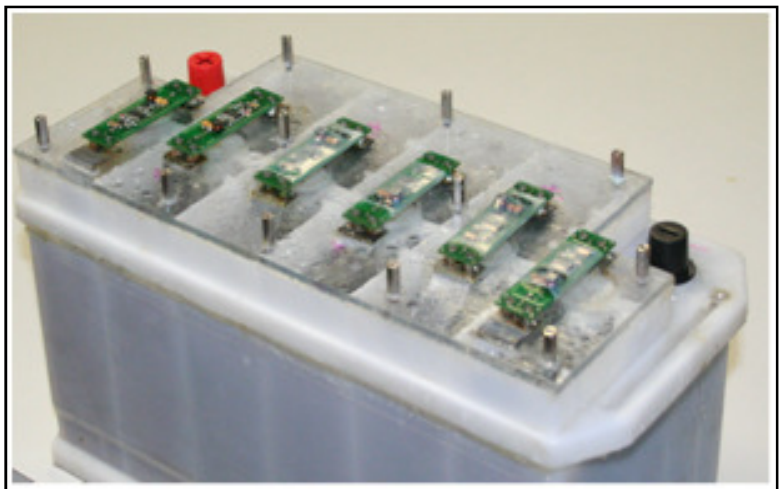

Figure 2: Sensors placed inside a rechargeable battery to monitor the individual cells (Matthias et al., 2015)

The SoC of a battery is the amount of charge available in a battery in percentage form at any given time in comparison to the same battery's charge when fully charged (Andrea, 2010). The SoH of a battery is a qualitative parameter that indicates the ability of the battery to deliver the charge that is stored in it at any given time as compared to the same ability when the battery was new (Escobar *et al*., 2015). The definition of SoH can either be based on the battery's capacity or it's internal resistance, depending on the specific application to which the battery is put (Caihao *et al*., 2013). There is no fixed definition for SoH and so battery manufacturers calibrate their own SoH thresholds and develop their own algorithms which then become part of their trade secrets (Rezvanizaniani *et al*., 2014).

2.2. Typical Battery Monitoring Methods

Any battery parameter that changes considerably and at times irreversibly with its usage such as internal resistance, water loss, grid corrosion and capacity loss, can be used for indicating the SoH of the battery (Anila *et al.*, 2014). The changes could be such as a rapid loss of power, internal degradations like passivation of the electrodes, sudden temperature rise in the battery, excessive gassing and corrosion all of which eventually lead to deviant battery performance.

The most common method of determining the SoC of a battery is the Coulomb Counting method in which the battery current while its charging or discharging is measured and using Equation 1, it's SoC is computed (Zou *et al.*, 2014):

$$SoC_t = SoC_{t_o} + \int_{t_o}^{t} \frac{\eta I}{C_n} dt \quad (1)$$

In Equation 1, SoC_t is the estimated SoC at time *t*; SoC_{t_o} is the initial SoC; η is the efficiency of the current; *I* is the current which is assumed to be positive during charging process and negative when discharging; and the nominal capacity of the battery is denoted by C_n (Zou *et al.*, 2014). In this method, the total capacity of the battery is assumed to be fixed and so it does not vary with the temperature, age and discharge current of the battery (Vepa, 2013).

A second method of monitoring the SoC of a battery is by use of the open circuit voltage method in which the battery's voltage is measured using a meter connected across its terminals. A 30-minute rest period is required in case the battery had been freshly charged to allow diffusion inside the battery to come to an end before the voltage readings are taken (Huggins *et al*., 2014). The value of the voltage obtained is then compared to the corresponding SoC value in a standard chart that correlates the open circuit voltage of the battery to the SoC.

Another method of determining SoC is by using a hydrometer to get the specific gravity of the electrolyte that is used in the battery. The specific gravity shows the concentration of the acid in the electrolyte and it correlates directly to the battery's SoC (Garche *et al.*, 2009). Once the value of the specific gravity is acquired, it's coresponding SoC is read of from a standard table that relates the SoC to the specific gravity. For a fully charged battery, the specific gravity lies between 1.230 and 1.330 depending on the chemical technology used (Garche *et al.*, 2009).

A battery's SoH can be computed using its temperature fluctuation while the battery is in use. The recommended temperature for normal operation of a battery is 25^{o}C and so a temperature rise far above this causes an increase in the rate of chemical reactions inside the battery by a factor of 2 for every 5.5^{o}C temperature rise (Garche *et al*., 2014). Consequently, the rate of self-discharge reactions and chemical degradation processes double as well (Garche *et al*., 2009).). Once the battery temperature is measured, an algorithm is developed for computing the SoH of the battery.

Another method for finding the SoH of a battery is by using electrochemical impedance spectroscopy. In this method, an alternating current is injected into the battery using a current injector such that an identifiable current of a specified frequency and magnitude flows and causes a resultant voltage drop across the battery under test (Bergveld *et al*., 2013). From the voltage and current measurements obtained, the impedance spectra are deduced and used to predict the SoH of the battery.

The coulomb counting method cannot account for the deteriorating SoC of the battery through ageing which will lead to inaccuracies in the SoC and SoH values obtained. The 30-minute rest period needed for the open circuit voltage method compromises the measurement accuracy because of voltage fluctuations and is unreliable for continuous battery monitoring. The specific gravity method is intrusive and cannot be used on sealed, maintenance free batteries. The electrochemical impedance spectroscopy method is expensive, time consuming and requires expertise in carrying it out and so, it is mostly reserved to research laboratories.

Generally, when the battery capacity drops to 80%, it is recommended that it be replaced (Xing *et al*., 2011). The failure modes of the LAB are dependent upon the type of application and the specific battery design for that application. Some cells inside the battery may deteriorate faster than others due to increase in resistance and accumulation of discharge products thereby reducing the voltage output of the battery (Chen *et al.*, 2012). The LAB has extremely low internal resistance of 0.022 Ohms per cell and so the voltage drop when current is drawn from it is remarkably small (Gianfranco, 2008). Internal short circuits in the battery formed by dendrites growth across the separators between the positive and the negative electrode during each battery cycle may lead to exothermic reactions and decreased capacity (Wu *et al*., 2014).

2.3. Present day Commercial Battery Monitors

The Bosch BLT 301 from Bosch Group in Germany is a hand-held battery tester used for testing 12V, 32Ah – 180Ah, lead-acid type automotive batteries by means of a fixed load. The test takes 5 seconds to determine the condition of the battery and displays the result as 'Good', 'Weak' or 'Bad' (de-ww.bosch-automotive.com, 2016).

Delphi Automotive, a company based in United Kingdom has developed the Delphi Battery Monitoring Device that calculates the SoC and SoH in order to control battery charging as well as to manage the car's electrical loads. It measures currents as high as 1500A via a 100μΩ shunt (www.delphi.com, 2016).

The Projector BLT 200 from Projector company in Australia is normally installed in the car such that it draws its power from the cigarette lighter on the car's dashboard and can monitor 12V and 24V automotive battery systems (www.projecta.com, 2016). The BLT 300 tester has four temperature calibrations of 21^{o}C, 10^{o}C, -1^{o}C and -18^{o}C from which the battery can be monitored. The ambient battery temperature is approximated to the closest scale from these four and thereafter the battery's voltage and current values are taken and used to compute the battery's SoH (www.projecta.com, 2016).

3. The Car Starting System

The car starting system comprises the battery, high current carrying cables and connecting wires, ignition key or switch, starter solenoid and or relay, starter motor, flywheel ring gear, starter drive and stator safety switch for automatic drive cars (Hollembeak, 2011)**.** The stator motor, shown in Figure 3 alongside other components, changes the electrical energy from the battery into mechanical energy.

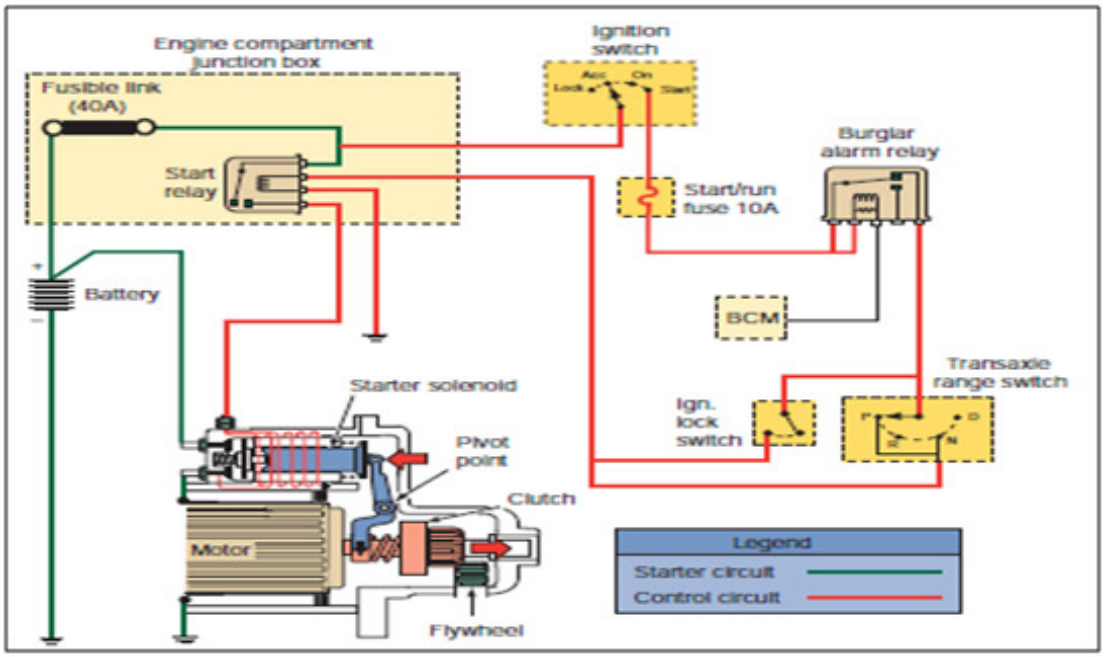

Figure 3: A simplified car starting system(Erjavec and Thompson, 2014)

The starter motor draws a large amount of current required to generate enough torque to turn the flywheel which in turn runs the engine (Gilles, 2012). The ignition system transforms the norminal 12 V of the battery to about 8kV to 40 kV and deliver it to the correct engine cylinder to ignite the compressed air and fuel vapor therein. When one winding of the ignition coil switches on and off it, causes a high voltage to be induced in the secondary winding (Denton, 2006). The starter motor can draw as high as 1500A on light duty vehicles and 2500A on commercial vehicles (Murugesan *et al*., 2012). Immediately after engine cranking, the voltage of the battery does not normally go back to its original value implying that there is a voltage loss (V_{loss}) associated with engine cranking events.

4. Design of the Battery Monitoring System

4.1. Introduction

The apparatus used in this research were a 500A battery load tester, a 1500cc Toyota Carina and the fabricated BMS. The block diagram in Figure 4 shows the system components and the working relationship between them. The direction of signals flow in the whole system is indicated by the arrows connecting those components. The specific function represented by each block is written inside that particular block.

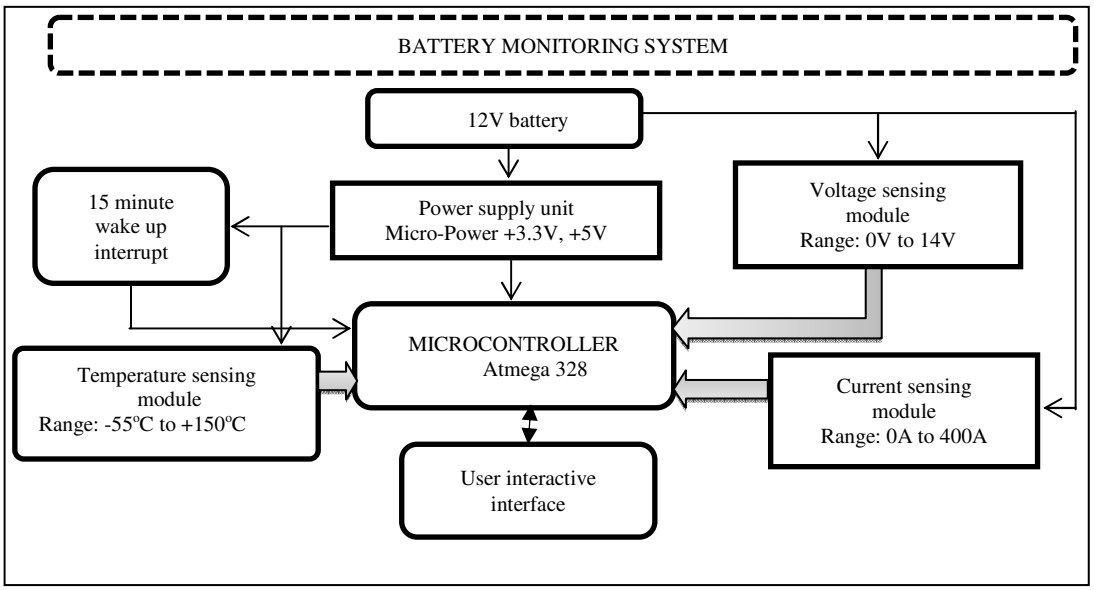

Figure 4: The block diagram of the battery monitoring system

4.2. The Battery Monitoring System Modules Design

The voltage divider theorem was used to design the voltage sensing module for measuring the voltage. A hall effect current sensor was used to measure the magnetic flux density generated around the current carrying conductor and convert it into a proportionate voltage. For measuring the temperature, a programmable digital thermal, DS18B20, probe was used. A voltage regulator was used to scale down the supply voltage of 12V to the required 5V for the current and temperature sensors and the Arduino microcontroller.

4.2.1. The voltage Sensing Module for Measuring the Battery Voltage

The voltage divider with two resistors, resistor 14 (R14) rated 100 kΩ and resistor 15 (R15) rated 10 kΩ connected in series as shown in Figure 5 was designed for measuring the battery's voltage. The voltage input (V_{in}) from the battery is applied across the two series resistors R14 and R15.

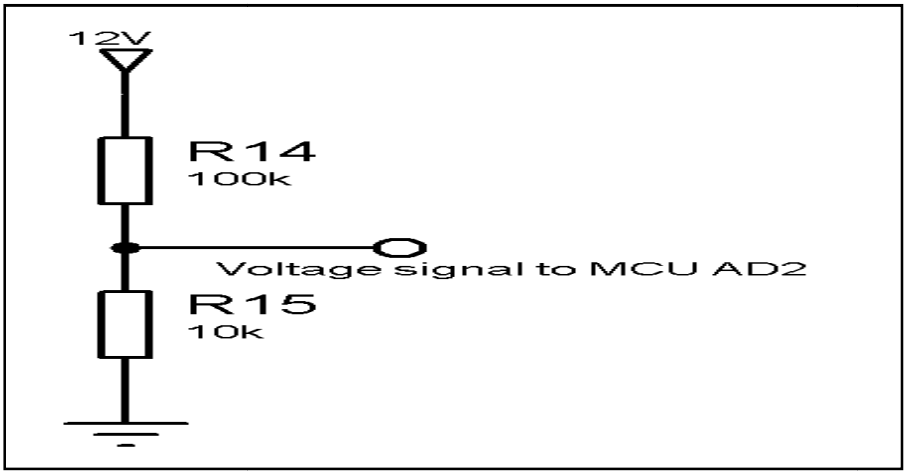

Figure 5: The voltage divider for measuring the battery voltage

The output voltage (V_{out}) across R15 is given by Equation 2 below (Raymond *et al*., 2009):

$$V_{out} = \frac{V_{in} \times R_{15}}{(R_{14} + R_{15})} \quad (2)$$

The analog voltage (V_a), measured is obtained based on Equation 3 below (Bayle, 2013):

$$V_a = \frac{5 \times \text{analogRead ( ) value}}{1023} \quad (3)$$

4.2.2. The Current Sensing Module for Measuring the Battery Current

The 5 pin ACS755SCB-200U current sensor from the Allegro family of current sensors was used for measuring the current drawn during engine cranking. Since one of this type of current sensors measures a maximum of 200A, two of them were connected in parallel so as to measure a current of up to 400A.

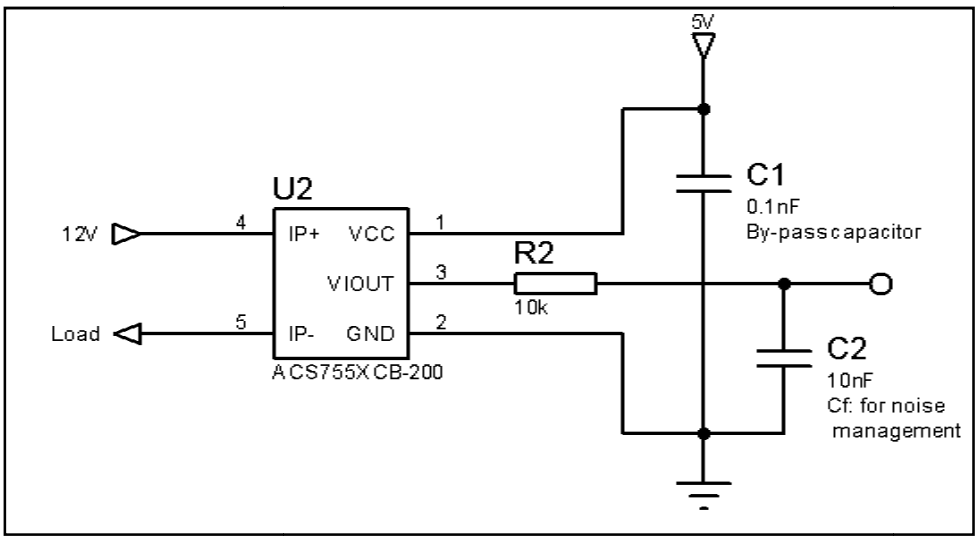

Figure 6: Current sensing module IC, ACS755SCB-200U, for measuring the battery current

When the current flows through the copper conductor, pin 4 and pin 5, in the current sensor shown in Figure 6, a magnetic field is generated around the conductor which is then converted into a proportionate voltage (Microsystems, 2016).

4.2.3. The Temperature Sensing Module for Measuring the Battery Temperature

The battery's temperature measurements were done using a digital thermal probe, DS18B20, which was attached to the side of the battery under test. The temperature sensor uses two voltage signals derived from bipolar transistors inside the digital temperature probe to generate a proportionate temperature measurement based on its voltage output. The circuit connection of DS18B20 is shown in Figure 7.

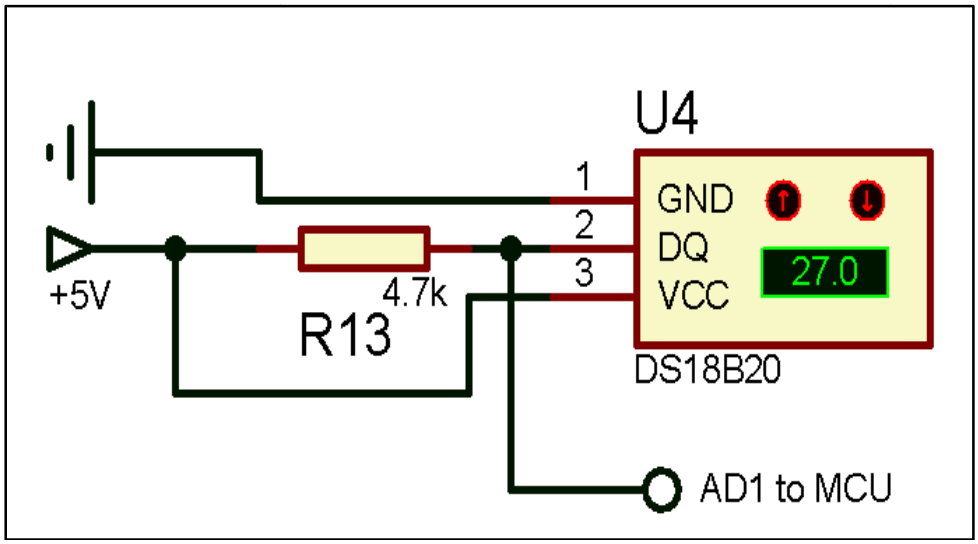

Figure 7: The digital temperature sensor, DS18B20 for measuring the battery temperature

4.2.4. Voltage Regulator Module for Stepping down Voltage from 12V to 5V

The LM 7805 IC was used as shown in Figure 8 to regulate the voltage supply from 12V to 5V to be used by the temperature and current sensors and the Arduino Uno R3 microcontroller unit.

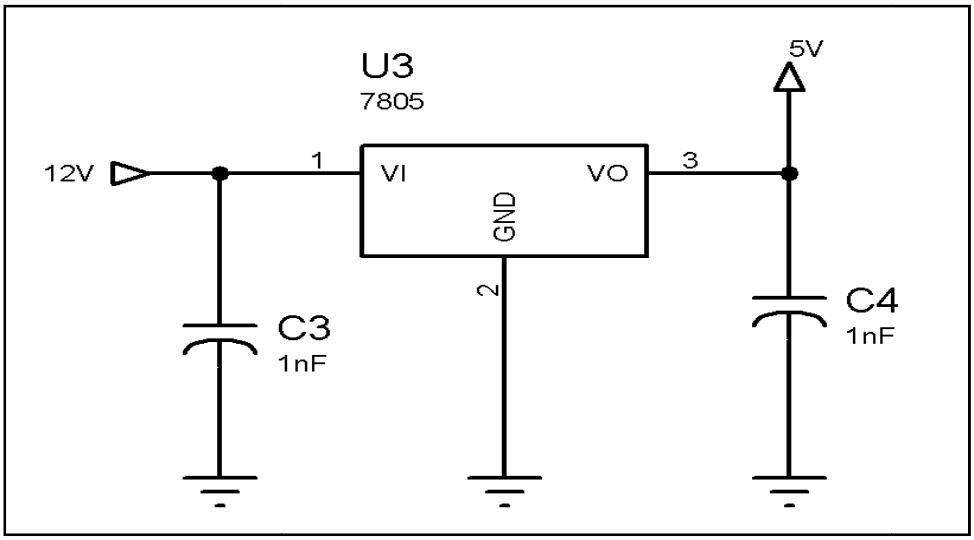

Figure 8: LM 7805 based voltage regulator for reducing the voltage from 12V to 5V

4.2.5. The User Interactive Interface

The user interactive interface shown in Figure 9 has Power and Reset button switches for turning on and resetting the BMS respectively and a Data hold button switch for prolonging the display time of the output on the screen.

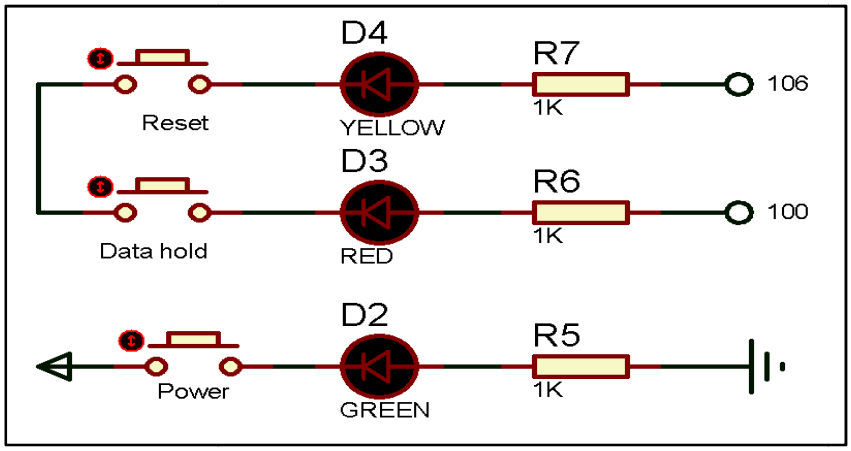

Figure 9: The user interactive interface

The computed output was displayed on a 160 x 128, 160 columns and 128 rows, arrays of the PG160128A thin film transistor screen.

4.2.6. The Data Logger for Storing the Measured and Computed Data

The secure data card for storing data was mounted on to the Arduino microcontroller compatible data-logger shield shown in Figure 10.

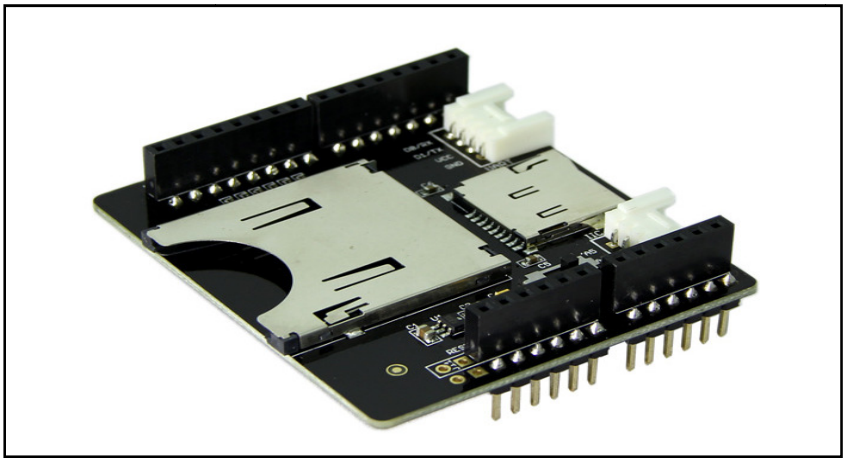

Figure 10: A stackable data logger with a secure data card slot (Igoe, 2011)

4.2.7. The Processing Unit for the Battery Monitoring System

The processing unit of the battery monitoring system is the Arduino Uno R3 programming board shown in Figure 11. The Arduino board was programmed using Arduino programming language which is a combination of C and C++ programming languages.

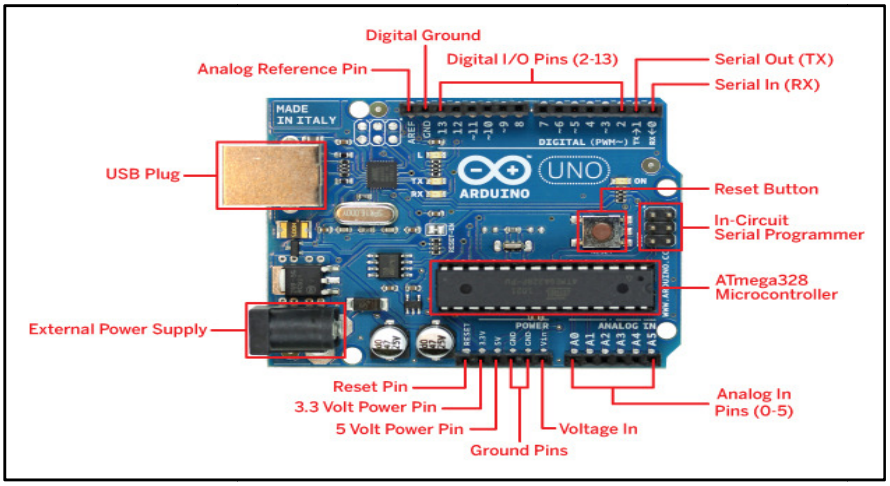

Figure 11: The Arduino Uno R3 board for processing the voltage, current and temperature signals (Banzi, 2011)

5. Fabrication of the Battery Monitoring System and the Engine Cranking Process

When the car ignition key is turned to the ON position, the battery's open circuit voltage and temperature are recorded. When the key is moved to the START position, the voltage and current values during engine cranking are taken and used to compute the SoH of the battery using Equations 4 to 12 that are embedded in the ATmega 328 microcontroller on the Arduino board. The computed data is displayed on the screen and simultaneously stored into the secure data card on the data logger.

5.1. Flow Diagram of the Battery Monitoring System

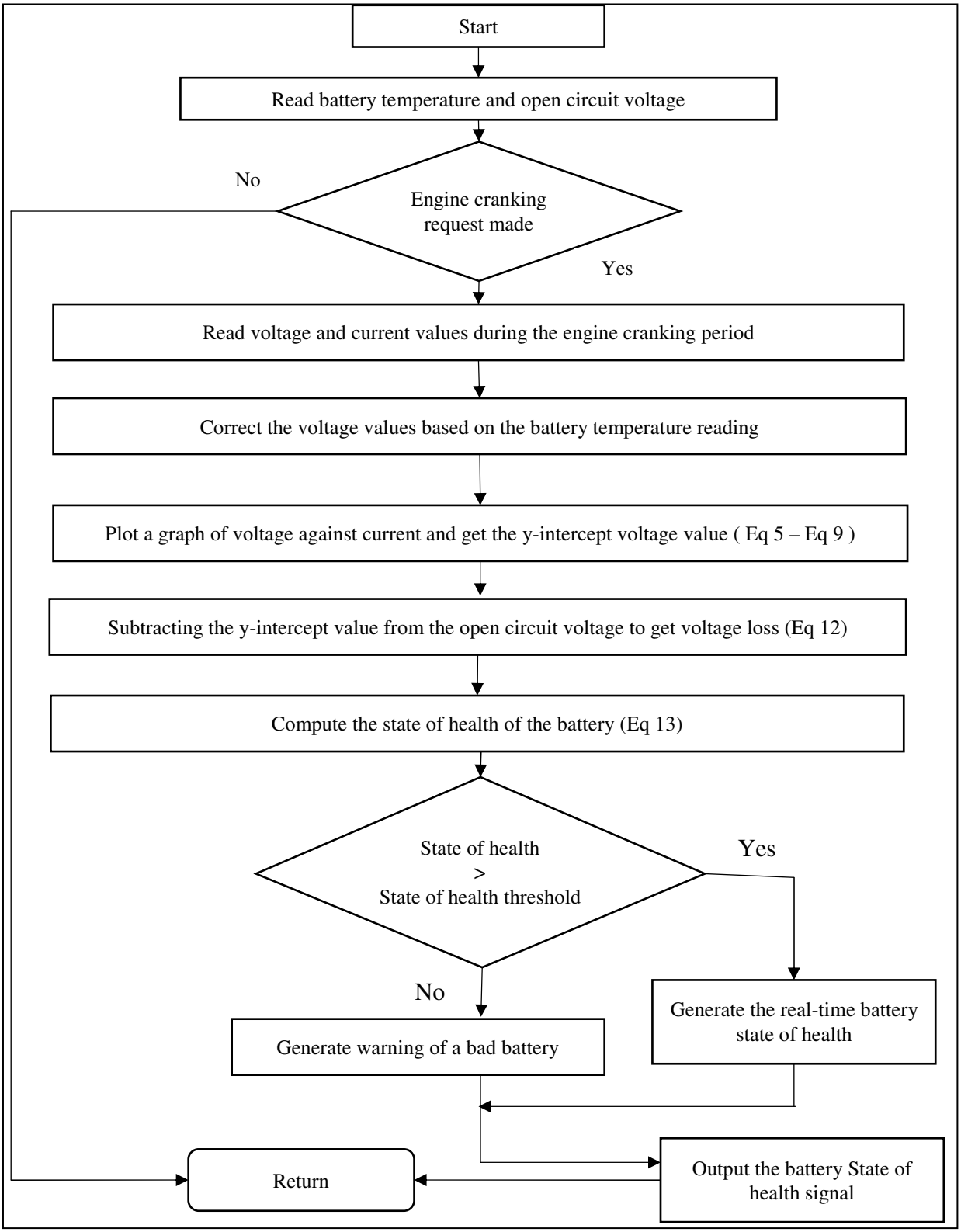

Figure 12:The flow diagram of the battery monitoring system

5.2. The State of Health Indication Algorithm for the Battery Monitoring System

Since the battery temperature affects the open circuit voltage (OCV) and performance of the battery, a temperature compensation algorithm was used to correct the OCV and other voltage values before using them to compute the state of heath of the battery. The V and I value are designated as **v** for voltage and **c** for current respectively for use in the linear regression formulae listed below from Equation 4 to Equation 12 (Ronald *et al*., 2004):

$$v = a + bc \quad (4)$$

where **a** is the y-intercept and **b** is the regression coefficient of **v** on **c**;

$$S_{cc} = \sum c^2 - \frac{(\sum c)^2}{n} \quad (5)$$

$$S_{vv} = \sum v^2 - \frac{(\sum v)^2}{n} \quad (6)$$

$$S_{cv} = \sum cv - \frac{\sum c \sum v}{n} \quad (7)$$

and

$$b = \frac{S_{cv}}{S_{cc}} \quad (8)$$

$$\text{y intercept } a = \bar{v} - b\bar{c} \quad (9)$$

the regression coefficient;

$$r = \frac{S_c}{\sqrt{S_{cc} S_{vv}}} \quad (10)$$

$$V = V_o + IR_{batt} \quad (11)$$

The voltage values obtained during engine cranking were plotted against the values of the corresponding current values and a line of best fit, which is described by the Equation 11 was plotted. Equation 11 is a linear equation, similar to the regression Equation 4 where V_o is the y-intercept value similar to **a,** and R_{batt} the battery resistance similar to the regression coefficient **b**. Plotting the graph was one way of getting the V_{loss}, and so in a second method of acquiring the same was applied by using the voltage and current values in equations 5 to 11 to compute the V_{loss}. After applying Equations 5 to 11, the V_{loss} was arrived at by using Equation 12;

$$V_{loss} = OCV - V_o \quad (12)$$

The values of SoC and V_{loss} acquired during the engine cranking event are then compared with the voltage loss threshold value, V_{lossth}, and SoC threshold, SoC_{th}, value. It is recommended that battery load testing be done when the battery's SoC is 75% but Spectro™ CA-12 battery tester from Cadex Inc. uses a minimal SoC of 60% (Buchman, 2016). To get the $SoC_{th,}$ it was assumed that the battery monitoring system had an error margin of 3% and another 1% due to parasitic losses and so the SoC_{th}wastaken to be 71%. To get the V_{lossth} and voltage loss of a new battery, $V_{lossnew}$, engine cranking was simulated in the laboratory using a 500A battery load tester on a brand-new battery from which the average V_{loss} and $V_{lossnew}$ were found. The tests on the LAB were therefore conducted with the following measured parameters and assumed theoretical thresholds;

i. $V_{lossnew} = 0.5V$
ii. $SoC_{th} = 71\%$
iii. $V_{lossth} = 1.5V$
iv. $SoH_{th} = 80\%$

The V_{loss}, temperature and SoC signals are used to compute the battery's SoH using Equation 13 below (Zhang, 2012);

$$SoH = \frac{V_{loss} - V_{lossth}}{V_{fresh} - V_{lossth}} \times 100 \quad (13)$$

The SoH index values that are less than zero are set at 0% while those that are greater than 1 are set at 100% (Zhang, 2012). The computed SoH is then displayed as a percentage in one of the 3 ways listed below with an indicative or instructive message to the motorist as;

SoH: 90-100 %: Good and a green LED on the BMS turns on
SoH: 81- 89 %: Fair and a yellow LED on the BMS turns on
SoH: 80%: Replace battery and a red LED on the BMS turns on

5.3. Battery Monitoring Systemset-up in the car

The BMS was set up in the car with its positive terminal connected directly to the positive terminal of the car's battery such that the current drawn from the battery went through the BMS. The negative terminal of the battery monitoring system was connected to the negative battery terminal in the car and the display and user interface placed on the car's dashboard.

6. Results and Discussion

Following each cranking event, the display format of the results on the screen of the BMS appeared as shown in Figure 13 below;

OCV: 12.69V
Voltage loss: 0.11 Volts
SoC: 100.00 %
SoH: 100.00 % ---> Health: Good
Battery Temperature: 85.00 Degrees Celsius
Cranking Duration: 0.59 Seconds

Figure 13: A sample display of the cranking results from the battery monitoring system

While the display will be showing the results in the format shown in Figure 13, the same results were simultaneously saved for each cranking event in an excel format in the data-logger of the BMS. The SoH and SoC for 78 engine cranking events using a brand new 75Ah Chloride Exide battery in the laboratory set-up using a 500A battery load tester is shown in Figure 14 below;

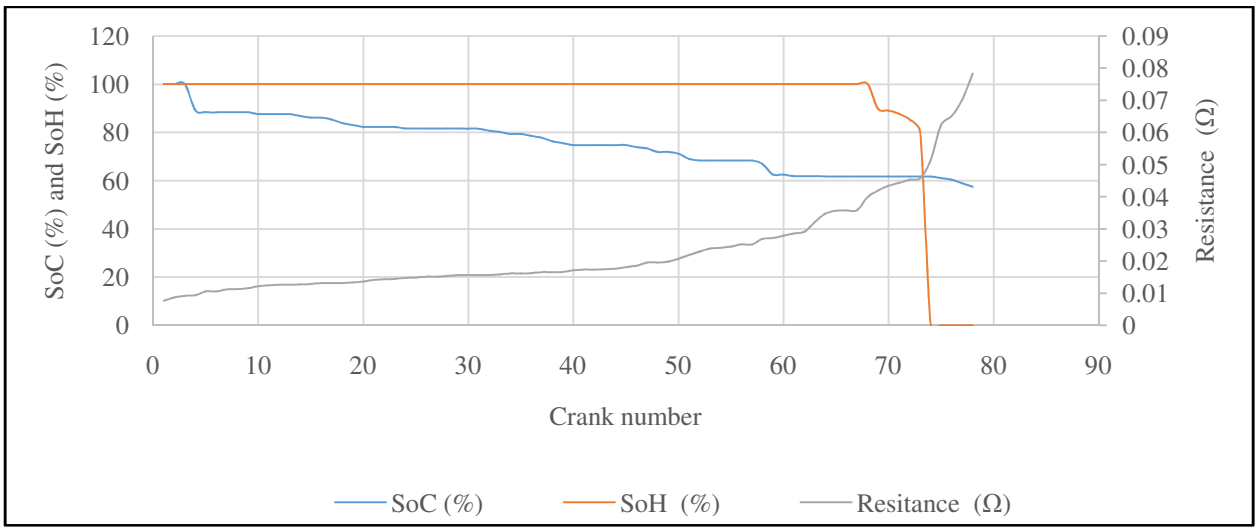

Figure 14: SoH and SoC against the number of cranks for a brand-new 75Ah Chloride Exide battery

At the crank number 68, the SoH fell below 100% and at crank number 73, it fell below the threshold value of 80%. The display for the crank number 74 to 78 showed that the battery should be replaced because the SoH had fallen below the 80% threshold. The SoC also kept on decreasing with every crank and gradually reduced to 57.42 %. The resistance of the battery kept increasing with each cranking event. This cranking events were simulated in the laboratory using a 500A battery load tester which drew a current ranging between 200A and 250A during every crank event. The battery was not charging during all these cranking events and that's why the SoC kept reducing.

The cranking data for the second battery, a 100Ah Unistar battery that had been used in a car for two years is shown in Figure 15.

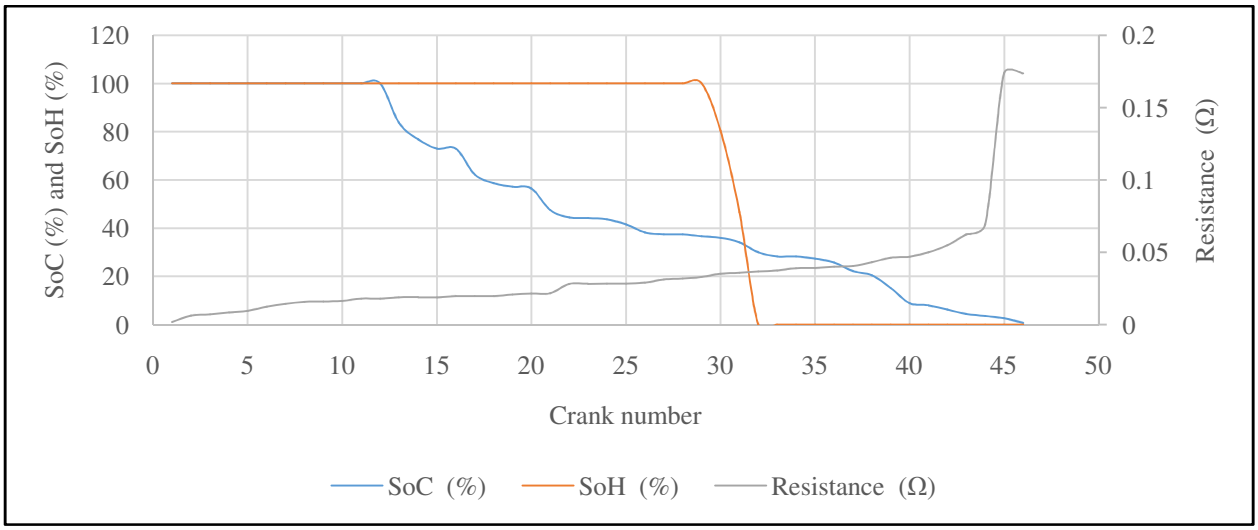

Figure 15: SoH and SoC against the number of cranks for a 2-year-old Unistar battery

The SoC and SoH for the Unistar battery were both 100% up until crank number 12 when the SoC started reducing. The SoH remained at 100% until crank number 29 and on crank number 30, it fell to 80.33%. At the failure point, that is crank number 31, the SoC was 34.02%, SoH 46.62 °C and the resistance 0.0358Ω. The range of resistance for the 47 cranking events was 0.0016Ω – 0.1735Ω. The SoC_{th} ,71%, was reached at crank number 16 and so the battery should have been charged at this point before proceeding with more cranking events but since the current being drawn from this battery was between 100A and 120A, the SoH was above threshold. There were 15 more successful cranks after the SoC_{th} value had been reached as can be seen from the corresponding SoH values reading 100%. This battery's health had deteriorated so much since it failed the crank test after 30 cranking events otherwise the SoC should have been above threshold for more than the recorded 16 cranks before starting to decrease. Since the battery cranked successfully below SoC threshold, it means that successful cranking depends on the magnitude of the load applied to the battery.

The Unistar battery was charged to 12.65V and installed in a 1500cc Toyota Carina for a period of one week to collect the cranking data. The acquired data is represented in the graph in Figure 16.

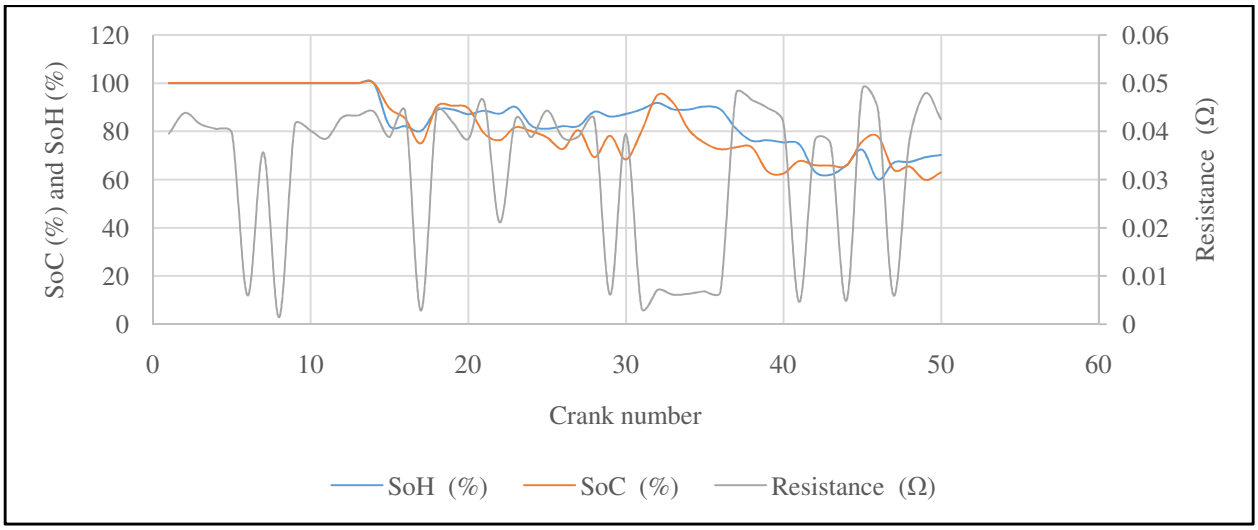

Figure 16: SoH and SoC against the number of cranks the 100Ah Unistar battery in a 1500cc Toyota Carina

With the Unistar battery installed in the car, 50 cranks were recorded with the first 25 taken over a distance of 5km moved by the car. The rest of the cranks were taken while the car was in a stationary condition. In the first 14 cranks, both the SoH and SoC was 100% and the car cranked in 0.56 seconds. From crank number 15 to crank number 25, the cranking time increased to an average of 0.72 seconds due to reduction of the SoC and an increase in battery resistance. The engine cranked successfully up to the point where the SoH was 75%, below which there was no successful cranking. The range of resistance for this battery when used in this car was 0.0014Ω – 0.0486Ω while the temperature was 33.31°C.

The brand-new Chloride Exide battery was charged to 12.65V and installed in the 1500cc Toyota Carina for five days and the cranking data collected is shown in Figure 17.

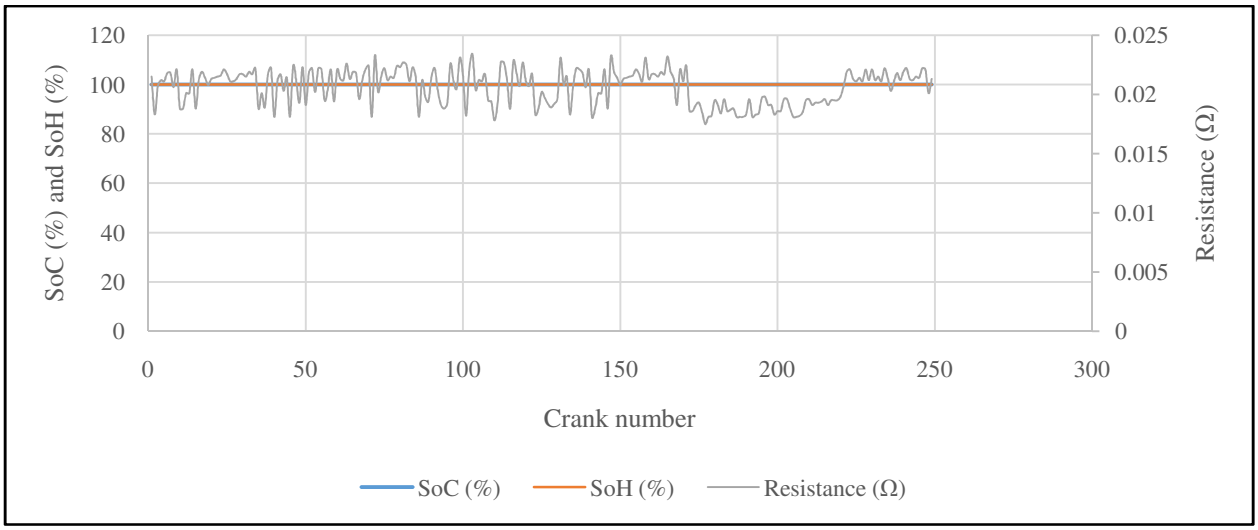

Figure 17: SoH and SoC for a brand-new 75Ah Chloride Exide battery in a 1500cc Toyota Corona

The SoC and SoH of the battery was 100% for the five days since the battery was brand new. The average cranking time was 0.49 seconds for each crank. The temperature of the battery was 23.7^{o}C for the first crank in the morning just before the car took off. The car covered an average of 102km on each day and the cranking data was taken when the temperature of the battery was 85^{o}C. The resistance of the battery was between 0.076Ω – 0.0783Ω.

7. Conclusions

The SoH of the SLI battery starts off at a high value and gradually decreases with battery usage. As the battery charging and discharging cycles increase, the battery's resistance increases and consequently lower the ability of the battery to crank the car. The battery degradation process takes place in the background such that the person using the battery, may not notice it. With the BMS installed in the car, the motorist will not need to wait for the battery to fail completely before replacing it. Most battery monitors found in cars only show the SoC of the battery, a parameter that cannot tell how healthy a battery is. The SoC and SoH monitoring using the developed BMS will monitor the electrical consumption of the loads in the car and help optimize the battery utilization and eliminate failures from unintended discharge. The BMS will also keep track of the ability of the battery to store and supply charge Motorists can use the new BMS in their cars to monitor their battery performance, conserve energy, save expensive battery repairs and avoid being inconvenienced by breakdowns from battery failures.

8. Recommendations

There gap between the laboratory tests and the real time field applications need to be narrowed down so as to develop more accurate monitoring devices. The voltage threshold value in this research was selected based on car engine cranking simulations in the laboratory using a 500A fixed load battery tester that takes 10 seconds whereas the actual average car cranking time was 0.59 seconds. The performance of the BMS under operating conditions, such as vibration from bumpy roads and temperature extremes from snow, rain or summer heat need to be studied so that these external loads will be reflected in the battery's available capacity. The BMS should be installed in a car for at least one year to be able to get a better deterioration trend of the starter battery in order to improve the accuracy of the SoH indication algorithm.

9. References

i. Bergveld, H. J. (2013). Battery Management System; Design and Modelling. Eindhoven,Nederlands: Royal Philips Electronics.
ii. Banzi, M. (2011). Getting Started with Arduino 2nd Eddition. Sebastopol, CA: O'Reilly & Associates.
iii. Buchman, I. (2016, 8 3). http://www.cadex.com/en/products/. Retrieved from http://www.cadex.com/en/: http://www.cadex.com/en/products/spectro-ca-12-ga
iv. Bosch, R. (2016, 12). http://www.boschdiagnostics.com. Retrieved from http://www.boschdiagnostics.com/pro/products/bat-110-battery-tester.
v. Chris K. Dyer, Patrick T. Moseley,Zempachi Ogumi,David A. J. Rand,Bruno Scrosati,. (2014).
vi. David Linden and Thomas B. Reddy. (2002). Handbook of Batteries. New York USA: McGraw Hill Companies Inc, 104-105.
vii. Delphi,Inc.(2016,August3).Retrieved September, 3,2016 from http://www.argusanalyzers/: http://forex.hu/images/pdf/ARGUS500.pdf
viii. Denton, T. (2006). Advanced automotive fault diagnosis second edition. Burlington, MA: Elsevier BH, 108-113.
ix. Florez-Escobar W. F., C. A. Brebbia, F. Chejne,F. Mondragon. (2015). Energy and Sustainability VI. Southampton SO40 7AA UK: WIT Press, 243-247.
x. Gilles, T. (2012). Automotive Service: Inspection, Maintenance, Repair. MA 02451, USA: Cengage Learning, 367.
xi. Huggins, R. (September 11, 2014). Energy Storage 2010 edition. New York: Springer.
xii. Hui Wu, Denys Zhuo, Deshang Kong, Yi Cui. (2014, 10 13). Improving battery safety by early detection of internal shorting with a bifunctional separator. Nature Communications, **5**, 5193.
xiii. http://www.projecta.com.au/Products/BatteryMaintenance/BatteryTesters.aspx. (2016, 8 3). Retrieved from http://www.projecta.com.au/site/DefaultSite/filesystem/documentshttp://www.projecta.com.au/site/DefaultSite/filesystem/documents/BatteryMaintenance/BLT300_Instructions_Issue1.pdf
xiv. Hollembeak, B. (2011). Automotive Electricity and Electronics, 5th edition. USA: Delmar cengage learning, 471.
xv. Jack Erjavec, Rob Thompson. (2014). Automotive Technology: A Systems Approach. NY USA: Cengage Learning, 543.
xvi. Jurgen Garche, Chris K Dyer, Patrick T, Mosley, Zempani Ogumi, David A.J. Rand, Bruno Scrosati. (2009). Encyclpedia of Electrochemical Power Sources. NX Amsterdam: Elsevier,556.
xvii. Jurgen Garche,Chris K. Dyer, Patrick T. Moseley,Zempachi Ogumi,David A. J. Rand,Bruno Scrosati. (2014).Encyclopedia of Electrochemical Power Sources,Amsterdam Netherlands: Elsevier, 729-795.
xviii. Joey Jung, L. Z. (2016). Lead-Acid Battery Technologies: Fundamentals, Materials, and Applications. Boca Raton Florida: CRC Press, 5-6.
xix. Matagne, D. R. (2012). Green Energy , Optimization of Photovoltaic Power Systems. London: Spinger.
xx. Matthias Schneider, S. I.-R. (2015). Vehicle Batteries with Wireless Cell Monitoring. IEEE, 3-4

xxi. Microsystems, A. (2016, June 30). http://www.allegromicro.com/. Retrieved from http://www.allegromicro.com/en/Products/Current-Sensor-ICs.aspx: http://www.allegromicro.com/en/Products/Current-Sensor-ICs/Fifty-To-Two-Hundred-Amp-Integrated-Conductor-Sensor-ICs.aspx

xxii. Raymond A Serway, Jerry S Faughn,Chris Vuille . (2009). College physics. Belmont, CA: Brooks/Cole, Cengage Learning, 570.

xxiii. Ronald E. Walpole,Raymond H. Myers,Sharon L. Myers,Keying Ye. (2004). Probability & Statistics for Engineers & Scientists EIGHTH E D I T I ON. Upper Saddle River, N.I 07458: Pearson Prentice Hall.

xxiv. S. N. Patil,Sangmeshwar S. Kendre, R. C. Prasad . (2011). Battery Monitoring System using

xxv. Thyagarajan Anila,Raja Prabu R., G. Uma. (2014-2-5). Battery Monitoring and Power Management for Automotive Systems. American Journal of Energy Research, 2(1), 1-8.

xxvi. Vepa, R. (2013-09-11). Dynamic Modeling, Simulation and Control of Energy Generation. London: Springer Science & Business Media, 325-327.

xxvii. Weng Caihao, Cui Yujia, Sun Jing, Peng Huei. (2013). On-board state of health monitoring of lithium-ion batteries using incremental capacity analysis with support vector regression. Journal of Power Sources, 36-44.

xxviii. Yinjiao Xing, Eden W. M. Ma,Kwok L. Tsui,Michael Petch. (2011). Battery Management Systems in Electric and Hybrid Vehicles. Energies, **4**,1840-1857.

xxix. Yalian Yang, Xiaosong Hu, Datong Qing, Fangyuan Chen. (2013). Arrhenius Equation-Based Cell-Health Assessment: Application to Thermal Energy Management Design of a HEV NiMH Battery Pack. Energies, 6(5), 2709-2725. doi:10.3390/en6052709

xxx. Yuan Zou,Xiaosong HU, Hongmin Ma,Shengbo Eben Li,. (2014). Combined State of Charge and State of Health estimation over lithium-ion battery cell cycle lifespan for electric vehicles. Journal of Power Sources, 273, 793-803.

xxxi. Yuasa, B. (2016, June 27). http://www.yuasabatteries.com/. Retrieved from http://www.yuasabatteries.com/pdfs/TechManual_2016.pdf: http://www.yuasabatteries.com/pdfs/Yuasa_Application_Guide_2016.pdf

xxxii. Zhang, X. (2012). "Battery State of Health Monitoring System And Method" Mason Ohio, USA Patent No. US 8,159,189 B2.

xxxiii. Pistoia, Gianfranco. (2008). Battery operated devices and systems: From portable electronics to industrial products. Rome: Elsevier.